

Magnetic Interaction in White Dwarf Binaries as Mechanism for Long-Period Radio Transients

YUANHONG QU ^{1,2,*} AND BING ZHANG ^{1,2,†}

¹*The Nevada Center for Astrophysics, University of Nevada, Las Vegas, NV 89154*

²*Department of Physics and Astronomy, University of Nevada Las Vegas, Las Vegas, NV 89154, USA*

ABSTRACT

A growing population of long-period radio transients has been discovered and their physical origin is still up to debate. Recently, a new such source named ILT J1101 + 5521 was discovered, which is in a white dwarf (WD) – M dwarf (MD) binary system, with the observed 125.5 min period being identified as the orbital period and the radio emission phase coinciding with the conjunction configuration when the MD is at the far end. We suggest that the radio emission properties of the system can be well explained within the framework of the unipolar inductor magnetic interaction model between the magnetized WD and the MD with low magnetization, with the electron cyclotron maser being the most likely radiation mechanism. This mechanism is similar to that of Jupiter decametric emission due to Jupiter-Io interaction. We suggest that this mechanism can interpret at least some long-period radio transients, especially the ultra-long period sub-population.

Keywords: binaries: close – radiation mechanisms: non-thermal

1. INTRODUCTION

Recently, a growing population of long-period radio transients (LPRTs) have been discovered (Hyman et al. 2005; Hurley-Walker et al. 2022, 2023, 2024; de Ruiter et al. 2024). These sources typically have a period from minutes to hours, usually with a duty cycle of the active window $\Delta t/P \ll 1$ (where Δt is the active duration and P is the period). The physical origin of these sources is unknown. The suggested engines include the spindown-powered magnetized white dwarf pulsars (Zhang & Gil 2005; Katz 2022), ultra-long-period magnetars (Wadiasingh et al. 2020), and regular magnetars with long-period precession (Zhu & Xu 2006). A related white dwarf optical pulsar source with the similar period has an M dwarf companion Marsh et al. (2016) and may be powered by binary interactions (Geng et al. 2016). Multi-wavelength observations have given constraints on some of these models (Kaplan et al. 2008; Rea et al. 2022, 2024), but there has been no smoking gun observational clue that helps to nail down the physical origin of these systems.

Recently, a newly discovered LPRT, named ILT J1101 + 5521, has been identified as a white dwarf (WD) – M dwarf (MD) system, and the measured ~ 125.5 -min period is identified as the orbital period (de Ruiter et al. 2024). Particularly, de Ruiter et al. (2024) found that the MD is behind the WD and in line with respect to Earth when the radio pulses are

emitted. Incidentally, two other long period transients, i.e. the 3.56-hr-period optical white dwarf pulsar AR Scorpii (Marsh et al. 2016) and the 2.9-hr-period LPRT GLEAM-X J0704-37 (Hurley-Walker et al. 2024), are also associated with an MD companion. It seems that WD – MD binaries likely provide the preferred physical conditions to produce pulsed emission in such systems at least for these sources.

In this paper, we propose that the coherent radio emission of ILT J1101 + 5521 is powered by a relativistic version of electron cyclotron maser mechanism in the magnetic field lines connecting the WD and the MD, with electromagnetic potential along the field lines excited through the unipolar inductor effect due to the orbital motion of the weakly magnetized MD moving in the magnetosphere of the magnetized WD. Such a mechanism has been successfully invoked to interpret the Jupiter decametric emission due to magnetic interactions between Jupiter and Io (Goldreich & Lynden-Bell 1969), and it has been speculated to also operate in other systems as well, including ultra-compact double white dwarf binaries (Wu et al. 2002; Dall’Osso et al. 2006), short-orbital-period extrasolar super-earths (Laine & Lin 2012), and binary neutron star or neutron star – black hole mergers (Hansen & Lyutikov 2001; McWilliams & Levin 2011; Lai 2012; Piro 2012; Wang et al. 2016). The paper is organized as follows. In Section 2, we discuss general constraints on physical models posted by the observations of ILT J1101 + 5521. In Section 3, we introduce the unipolar inductor magnetic interaction model and apply it to ILT J1101 + 5521. In Section 4, we discuss various radiation mechanisms for ILT J1101 + 5521

* E-mail: yuanhong.qu@unlv.edu

† E-mail: bing.zhang@unlv.edu

and conclude that electron cyclotron maser emission is the most likely candidate. In Section 5 we discuss other LPRTs and suggest that the ultra-long-period sub-population of these sources may share the similar physical origin. The results are summarized in Section 6.

2. GENERIC OBSERVATIONAL CONSTRAINTS

We first discuss some generic constraints on any physical model based on the observational results of ILT J1101 + 5521:

(i) The observed period ~ 125.5 min is consistent with the orbital period of the WD – MD binary system, with the radio pulses observed when the two stars are in conjunction and the MD is on the far side (de Ruiter et al. 2024). One can then estimate the semimajor axis of the binary as

$$a = (GM)^{1/3} \left(\frac{P}{2\pi} \right)^{2/3} \quad (1)$$

$$\simeq (5.3 \times 10^{10} \text{ cm}) \left(\frac{M}{0.8M_\odot} \right)^{1/3} \left(\frac{P}{125.5 \text{ min}} \right)^{2/3},$$

where $M = M_\star + M_c$ is the total mass of the binary system, and the characteristic values of $M_\star = 0.6M_\odot$ and $M_c = 0.2M_\odot$ are taken for the WD and the MD, respectively, following de Ruiter et al. (2024). The separation between the two stars ranges from $a(1 - e)$ to $a(1 + e)$, where e is the eccentricity. The orbit is close to a circle for this source (de Ruiter et al. 2024), thus $e \simeq 0$.

(ii) The peak flux density ranges from ~ 41 mJy to ~ 256 mJy with the pulse time duration Δt lasting between 30 to 90 seconds. The observed range of the radio pulse frequency is from 120 MHz to 168 MHz (de Ruiter et al. 2024). The brightness temperature can be estimated based on the observed parameters as

$$T_b = \frac{S_\nu D^2}{2\pi k_B (\nu \Delta t)^2} \simeq (3.9 \times 10^{13} \text{ K}) \left(\frac{S_\nu}{0.1 \text{ Jy}} \right) \quad (2)$$

$$\times \left(\frac{\nu}{140 \text{ MHz}} \right)^{-2} \left(\frac{\Delta t}{60 \text{ s}} \right)^{-2} \left(\frac{D}{504 \text{ pc}} \right)^2,$$

where S_ν is the flux density, ν is the typical frequency, and D is the distance. The maximum brightness temperature for incoherent radio emission can be estimated as (Zhang 2023)

$$T_{b,\text{incoh}} \simeq \Gamma \gamma m_e c^2 / k_B \simeq (5.9 \times 10^{11} \text{ K}) \Gamma \gamma_2, \quad (3)$$

where Γ and γ are the bulk motion Lorentz factor and the typical electron Lorentz factor, respectively. For the binary system we are interested in, there is no bulk relativistic motion of the emitter, so we only normalize the electron Lorentz factor to 100. Since $T_b \gg T_{b,\text{incoh}}$, the radio emission must be coherent.

(iii) Since radio emission is only detected in certain orbital phases, the coherent radio emission must not be isotropically

emitted. Geometric or relativistic beaming are needed (see Figure 1 for a possible geometry). The observed emission has high polarization, with the highest linear polarization degree $\sim 51\%$ for the brightest pulse and the circular polarization degree $< 1.6\%$ and $< 4.2\%$ for specific pulses (de Ruiter et al. 2024). These polarization properties are likely produced by relativistically moving electrons.

3. THE MAGNETIC INTERACTION MODEL

3.1. Physical picture

We consider a binary system consisting of a magnetized WD primary star with mass M_\star , radius R_\star , angular velocity Ω_\star and magnetic dipole moment $\mu = B_\star R_\star^3$. The companion MD star is non-magnetized with mass M_c and radius R_c . The distance between the two stars is a . The angular velocity of the WD is $\Omega_\star = \xi \Omega$, where the orbital angular velocity is $\Omega = 2\pi/P$ (P is the orbital period).

We first show that the WD carries a force-free magnetosphere. The gravitational force on a proton at the WD surface can be estimated as

$$F_{\text{grav}} = \frac{GM_\star m_p}{R_\star^2} \quad (4)$$

$$\simeq (2.7 \times 10^{-16} \text{ dynes}) \left(\frac{M_\star}{0.6M_\odot} \right) \left(\frac{R_\star}{0.01R_\odot} \right)^{-2}.$$

The electric force on one proton at the WD surface, on the other hand, may be calculated as

$$F_{\text{EM}} = \frac{q\Omega_\star R_\star B_\star}{c} \quad (5)$$

$$\simeq (9.3 \times 10^{-8} \text{ dynes}) \xi \left(\frac{P}{125.5 \text{ min}} \right)^{-1} \left(\frac{R_\star}{0.01R_\odot} \right) \left(\frac{B_\star}{10^7 \text{ G}} \right).$$

One can see that $F_{\text{EM}} \gg F_{\text{grav}}$ is satisfied, justifying a magnetically dominated magnetosphere similar to pulsar magnetospheres. The radius of the WD magnetosphere light cylinder can be estimated as

$$R_{\text{LC}} = \frac{c}{\Omega_\star} \simeq (3.6 \times 10^{13} \text{ cm}) \xi^{-1} \left(\frac{P}{125.5 \text{ min}} \right) \gg a \quad (6)$$

if $\xi \ll 10^3$. This suggests that the companion MD star is inside the magnetosphere of the WD.

We consider a toy model with Ω_\star and Ω aligned. The non-magnetized MD moving with respect to the WD magnetosphere would generate an electric potential drop of the magnitude of $\Phi \simeq 2R_c |\vec{E}|$ due to the unipolar induction effect. Here the factor of two is included since the circuit is repeated in both hemispheres. The induced electric field is

$$\vec{E} = \frac{\vec{v}}{c} \times \vec{B}_{\text{bg}}, \quad (7)$$

where $\vec{v} = |\vec{\Omega}_\star - \vec{\Omega}| \times \vec{r} = \Delta\Omega r \hat{\phi}$ is the companion star's velocity relative to the WD magnetosphere. The background

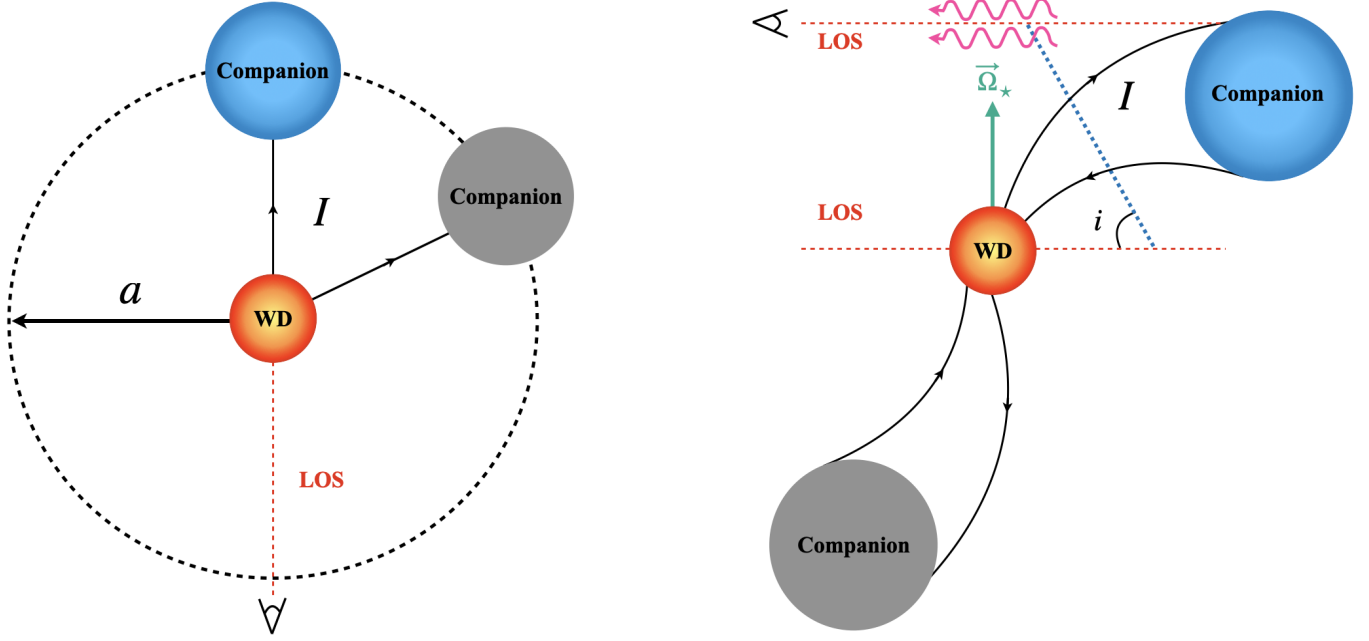


Figure 1. The geometric sketch of the WD-MD unipolar induction magnetic interaction model. The left panel is the top view and the right panel is the side view. The blue and black companion denote the configurations with and without observed radio emission, respectively. The radio emission (purple wiggler) is produced by relativistic particles in the magnetic loop connecting the two stars. The line of sight (LOS) is denoted as red dashed line. The inclination angle i is defined as the angle between the LOS and orbital plane normal vector. The separation distance between the WD and companion star is a .

dipole magnetic field strength at the separation distance can be estimated as

$$B_{\text{bg}} = B_{\star} \left(\frac{R_{\star}}{a} \right)^3 \approx (22 \text{ G}) \left(\frac{B_{\star}}{10^7 \text{ G}} \right) \left(\frac{R_{\star}}{0.01 R_{\odot}} \right)^3 \times \left(\frac{M}{0.8 M_{\odot}} \right)^{-1} \left(\frac{P}{125.5 \text{ min}} \right)^{-2}. \quad (8)$$

We can then obtain the total voltage when the two stars are at a separation of a (Lai 2012; Piro 2012)

$$\Phi \approx \frac{2\mu R_c}{ca^2} \Delta\Omega \approx (9.3 \times 10^8 \text{ statvolt}) \zeta \left(\frac{B_{\star}}{10^7 \text{ G}} \right) \left(\frac{R_c}{0.2 R_{\odot}} \right) \times \left(\frac{M}{0.8 M_{\odot}} \right)^{-2/3} \left(\frac{P}{125.5 \text{ min}} \right)^{-7/3}, \quad (9)$$

where

$$\Delta\Omega = |\Omega - \Omega_{\star}| = |\Omega - \xi\Omega| = |1 - \xi|\Omega = \zeta\Omega. \quad (10)$$

Notice that the star can spin faster or slower than the orbit, i.e. $0 < \xi \leq 1$ or $\xi > 1$, but $\zeta > 0$ is always satisfied because $\Delta\Omega$ is defined as the absolute value of Ω_{\star} and Ω difference. The current in the circuit may be calculated as $I = \Phi/2\mathcal{R}_{\text{mag}}$, where $\mathcal{R}_{\text{mag}} = 4\pi/c$ is the resistance of the magnetosphere. One can then estimate the total electric power dissipation rate

of the binary system as (Lai 2012; Piro 2012)

$$\dot{E}_{\text{diss}} = \frac{2\Phi^2}{\mathcal{R}_{\text{mag}}} \approx \frac{4\mu^2 R_c^2}{ca^4 \pi} \Delta\Omega^2 \approx (2.1 \times 10^{27} \text{ erg s}^{-1}) \zeta^2 \times \left(\frac{B_{\star}}{10^7 \text{ G}} \right)^2 \left(\frac{R_c}{0.2 R_{\odot}} \right)^2 \left(\frac{M}{0.8 M_{\odot}} \right)^{-4/3} \left(\frac{P}{125.5 \text{ mins}} \right)^{-14/3}. \quad (11)$$

The highest observed specific radio luminosity is $\sim 7.8 \times 10^{19} \text{ erg s}^{-1} \text{ Hz}^{-1}$ (de Ruiter et al. 2024). One can see that the model can satisfy this constraint if $B_{\star} > 2 \times 10^7 \text{ G}$ for $\zeta = 1$. In reality, it is possible that $\Omega_{\star} > \Omega$ (or $\zeta > 1$). This would increase the angular velocity difference which would further reduce the required B_{\star} .

3.2. Geometric configuration

Within this model, the particle flow that powers radio emission should be confined in the magnetic loop connecting the two stars. As a result, coherent radio emission can be only detected when the magnetic loop plane aligns with the line of sight, i.e. at conjunction (see Fig. 1 left panel for the top view of the orbit). In order to suppress emission from other phases, the radiating electrons are required to move relativistically. The fact that radio emission is observed when the MD is at the superior conjunction requires that the WD is an anti-parallel rotator, i.e. $\Omega \cdot \mu < 0$.

In the conjunction configuration alone cannot guarantee the detection of radio emission. Because of the relativistic motion of the particles, the emission beam is essentially along

the tangential direction of the field lines. Radio emission can be observed only when the magnetic field line tangential direction directions are close to the observer. Figure 1 right shows the side view of the system, with a marginal case that the field tangential direction barely reaches the line of sight. When the orbital inclination angle i is even smaller (e.g. close to the face on configuration), no coherent radio emission can reach the observer. Optical observations give the constraint that $i < 74^\circ$ and $i > 50^\circ$ from the observed radial velocity amplitude (de Ruiter et al. 2024). Our model provides another limit from the low end, with the minimum i depending on the unknown angle between Ω_\star and μ .

4. RADIATION MECHANISM

So far we have not specified the radiation mechanism. In this section, we survey various mechanisms and suggest that a relativistic version of electron cyclotron maser emission (ECME) is likely the emission mechanism.

4.1. Characteristic frequencies

We first study the relevant physical parameters in the WD magnetosphere. Since the WD magnetosphere can be treated as force-free, we can define a Goldreich–Julian (GJ) density (Goldreich & Julian 1969) for the WD

$$n_{\text{GJ}} = \frac{B_\star \Omega_\star}{2\pi qc} \left(\frac{r}{R_\star}\right)^{-3} \simeq (3.1 \times 10^{-2} \text{ cm}^{-3}) \xi \left(\frac{B_\star}{10^7 \text{ G}}\right) \times \left(\frac{P}{125.5 \text{ min}}\right)^{-1} \left(\frac{r}{10^{10} \text{ cm}}\right)^{-3} \left(\frac{R_\star}{0.01 R_\odot}\right)^3. \quad (12)$$

The plasma frequency corresponding to the GJ-density can be estimated as

$$\omega_p = \sqrt{\frac{4\pi q^2 n_{\text{GJ}}}{\gamma m_e}} \simeq (9.9 \times 10^2 \text{ rad s}^{-1}) \xi^{1/2} \left(\frac{B_\star}{10^7 \text{ G}}\right)^{1/2} \times \left(\frac{P}{125.5 \text{ min}}\right)^{-1/2} \left(\frac{r}{10^{10} \text{ cm}}\right)^{-3/2} \left(\frac{R_\star}{0.01 R_\odot}\right)^{3/2} \left(\frac{\gamma}{10^2}\right)^{-1/2}. \quad (13)$$

On the other hand, the electron cyclotron frequency can be estimated as

$$\omega_B = \frac{eB_\star}{m_e c} \left(\frac{R_\star}{r}\right)^3 \simeq (5.9 \times 10^{10} \text{ rad s}^{-1}) \left(\frac{B_\star}{10^7 \text{ G}}\right) \times \left(\frac{R_\star}{0.01 R_\odot}\right)^3 \left(\frac{r}{10^{10} \text{ cm}}\right)^{-3}. \quad (14)$$

For typical parameters, one has $\omega_B \gg \omega \gg \omega_p$.

4.2. Disfavored mechanisms

We survey various emission mechanisms and can rule out the following mechanisms.

- The required specific viewing geometry and the observed high linear polarization degrees suggest that the emitting electrons should be relativistic. This rules out the emission mechanisms invoking non-relativistic electrons, such as the non-relativistic version of the ECME.
- Type III solar flares emit coherent radio emission via collective Langmuir wave plasma emission (Melrose 2017). For a static plasma, the required plasma number density is $\sim 10^7 \text{ cm}^{-3}$ in order to have ω_p reach the observed frequency at $\sim 100 \text{ MHz}$. This density is much greater than the GJ-density. So at least the non-relativistic plasma emission is not suitable to explain the observations. More complicated relativistic plasma emission may be possible, but it is unclear how an instability can be driven from such a system.
- Relativistic electrons can radiate in the background magnetic field via synchrotron radiation or curvature radiation. The cooling timescale of synchrotron radiation can be estimated as

$$t_{\text{syn}} = \frac{6\pi m_e c}{\gamma \sigma_T \beta^2 B_{\text{bg}}^2} \simeq (3.3 \times 10^5 \text{ s}) \left(\frac{\gamma}{5}\right)^{-1} \left(\frac{B_\star}{10^7 \text{ G}}\right)^{-2} \times \left(\frac{M}{0.8 M_\odot}\right)^2 \left(\frac{P}{125.5 \text{ min}}\right)^4 > P = 7530 \text{ s}. \quad (15)$$

One can see that because the B field is not strong, the synchrotron cooling time is longer than the orbital period so that electrons cannot completely lose their perpendicular momenta. So curvature radiation is not relevant. For synchrotron radiation, the characteristic frequency $\omega_{\text{c,syn}} \sim \gamma^2 \omega_B$ is too high, because ω_B already exceeds the observed frequency for typical parameters (Eq.(14)). We therefore conclude that both synchrotron and curvature radiation are likely not the radiation mechanisms of these systems.

4.3. Relativistic electron cyclotron maser emission

We believe that a relativistic version of the ECME mechanism is likely operating in the system to power the observed coherent radio emission. Such a radiation emission mechanism (Twiss 1958) has been widely accepted to interpret decametric emission from Jupiter and auroral kilometric radiation from Earth. The Jupiter emission is triggered by the similar unipolar induction mechanism due to Jupiter-Io interaction (Goldreich & Lynden-Bell 1969). Three physical conditions are required to produce ECME: The first is population inversion of the energetic electrons in the direction perpendicular to the background magnetic field to achieve negative absorption, i.e. $\partial f / \partial p_\perp > 0$, where f is the particle distribution function and p_\perp is the momentum perpendicular

to the background magnetic field. The second condition requires $\omega_B \gg \omega_p$, which is satisfied here. Finally, one should satisfy the gyromagnetic resonance condition, which can be written as (Wu & Lee 1979; Melrose 2017)

$$\omega - s \frac{\omega_B}{\gamma} - k_{\parallel} v_{\parallel} = 0, \quad s = 0, \pm 1, \pm 2 \dots, \quad (16)$$

where s is the harmonic number, k_{\parallel} and v_{\parallel} denote the wave vector and velocity of the electron along the background magnetic field. We consider the case of $s = 1$. The emission frequency can be estimated as

$$\begin{aligned} \omega \simeq \frac{\omega_B}{\gamma} \simeq (5.9 \times 10^8 \text{ MHz}) \left(\frac{B_{\star}}{10^7 \text{ G}} \right) \left(\frac{r}{10^{10} \text{ cm}} \right)^{-3} \\ \times \left(\frac{\gamma}{10^2} \right)^{-1} \left(\frac{R_{\star}}{0.01 R_{\odot}} \right)^3, \end{aligned} \quad (17)$$

which is consistent with the typical frequency observed in ILT J1101 + 5521.

The observed emission of ILT J1101+5521 is mostly linearly polarized but also carries circular polarization. The non-relativistic version of ECME gives dominant circularly polarized emission. Linear polarization can be observed only in the direction perpendicular to the magnetic field line. We invoke a relativistic version of the ECME mechanism with electrons moving with $\gamma \sim 100$. The direction of the dominant linear polarization is at $1/\gamma \sim 0.01$ with respect to the electron motion direction. The observation is consistent with the line of sight slightly deviates from the tangential direction of the magnetic field lines.

Since cyclotron emission has a characteristic frequency, one prediction of the ECME mechanism is that the spectrum is expected to be narrow if γ is small (otherwise the spread of γ would broaden the spectrum). A lower γ also suggests a stronger circular polarization. We therefore predict an anti-correlation between the broadness of the spectrum and the degree of circular polarization Π_V . Future detection of LPRTs with narrow spectra and high Π_V will bring direct support to our model.

5. OTHER SOURCES

We have shown that the proposed magnetic interaction model invoking a WD – MD binary can successfully explain the observations of ILT J1101+5521. We suspect that the same model may apply to at least some of the other LPRTs as well, but probably with different parameters and observational geometric configurations. In the following, we discuss whether other reported LPRTs and related objects (Table 1) comply with the framework of our model.

- Besides ILT J1101 + 5521 (de Ruiter et al. 2024), the most likely candidate that has the similar origin is the recently detected GLEAM-X J 0704-37 with a 2.9-hour

period (Hurley-Walker et al. 2024). The polarization behavior of the source is variable with non-negligible linear (20–50%) and circular polarization (10–30%) over millisecond timescales. Optical observations revealed an MD counterpart (Hurley-Walker et al. 2024). Deeper observations will reveal whether the MD is in a binary system with a WD companion.

- A very relevant system is the optical white dwarf pulsar AR Scorpii (Marsh et al. 2016). The optical emission can be understood within the framework of a binary interaction model invoking a bow shock between the WD and MD winds (Geng et al. 2016). It is likely that AR Scorpii and ILT J1101+5521 belong to very similar systems. The different apparent behaviors may be attributed to the longer period of AR Scorpii that gives a lower unipolar interaction power, and also possibly an unfavored geometry (e.g. a smaller inclination angle) that does not permit the radio emission to enter the line of sight.
- The first long-period radio source was a transient source named GCRT J1745–3009 with a period of 77 minutes (Hyman et al. 2005). Motivated by the suggestion that the source could be a WD pulsar in the pair-production death valley (Zhang & Gil 2005), Kaplan et al. (2008) performed a deep search in the optical/infrared band and placed a 3σ limiting magnitudes from four bands: $I > 26$, $J > 21$, $H > 20$ and $K > 19$. This rules out the existence of a WD if the source distance is < 1 kpc. This source can be understood within our model if it is located at a distance larger than 1 kpc. The source was only briefly detected for a few periods. It could be understood if the line of sight is barely grazing the magnetic loop. Re-detection of the source during its next reactivation phase will help to test this model.
- GLEAM-X J1627-52 with a period of 18.18 minutes (Hurley-Walker et al. 2022) and GPM J1839-10 with a period of 21 minutes (Hurley-Walker et al. 2023) are two relatively fast LPRTs. Their emissions have polarization properties more similar to pulsars, e.g. high linear polarization ($\Pi_L \sim 88\%$) for GLEAM-X J1627-52 (Hurley-Walker et al. 2022) and $\Pi_L \sim 10\% - 100\%$ for GPM J1839-10 (Hurley-Walker et al. 2023), as well as flat polarization angle with occasional 90° jumps. Deep searches for optical counterparts gave inconclusive results (Rea et al. 2022; Hurley-Walker et al. 2023). These two sources are least likely consistent with our WD – MD interaction model and may have a different origin.
- ASKAPJ193505.1+214841.0 was reported to have a period of 53.8 minutes (Caleb et al. 2024). The po-

larization properties are highly variable: a bright pulse state with highly linear polarization ($> 90\%$) and a weak pulse state (~ 26 times fainter than the bright state) with highly circular polarization. There is a near IR source in the field, but whether it is associated with the radio emitter is uncertain. Further observations are needed to establish whether the IR source is an MD associated with the LPRT, and whether the source could be understood within the framework of the WD – MD interaction model.

6. CONCLUSIONS

In this paper, we propose a magnetic interaction model invoking a magnetized WD and a non-magnetized MD through the unipolar induction effect to interpret the newly discovered LPRT, ILT J1101+5521. We argue that a relativistic version of the electron cyclotron maser emission is the most likely emission mechanism. This is a more energetic version of the Jupiter-Io interaction observed in the solar system.

We further explore the possibility of applying this model to the emergent LPRT population with a rapidly growing

number. We find that those with relative long periods such as GLEAM-X J0704-37 and GCRT J1745-3009 and probably ASKAPJ193505.1+214841.0 as well, may be interpreted within the same theoretical framework. The WD optical pulsar AR Scorpii may also belong to the same type of system with a different evolution stage or viewing geometry. However, we note that the sources with relatively shorter periods, such as GLEAM-X J1627-52 and GPM J1839-10, do not seem to meet the model predictions and may have a different physical origin, e.g. a single WD pulsar or a long-period magnetar. More multi-wavelength observations of these systems and new sources will help to test the suggested dichotomy and the unified picture of the ultra-long period sub-population of LPRTs.

ACKNOWLEDGEMENTS

This work is supported by the Nevada Center for Astrophysics, NASA 80NSSC23M0104 and a Top Tier Doctoral Graduate Research Assistantship (TTDGRA) at University of Nevada, Las Vegas.

REFERENCES

- Caleb, M., Lenc, E., Kaplan, D. L., et al. 2024, *Nature Astronomy*, doi: [10.1038/s41550-024-02277-w](https://doi.org/10.1038/s41550-024-02277-w)
- Dall’Osso, S., Israel, G. L., & Stella, L. 2006, *A&A*, 447, 785, doi: [10.1051/0004-6361:20052843](https://doi.org/10.1051/0004-6361:20052843)
- de Ruiter, I., Rajwade, K. M., Bassa, C. G., et al. 2024, arXiv e-prints, arXiv:2408.11536, doi: [10.48550/arXiv.2408.11536](https://doi.org/10.48550/arXiv.2408.11536)
- Geng, J.-J., Zhang, B., & Huang, Y.-F. 2016, *ApJL*, 831, L10, doi: [10.3847/2041-8205/831/1/L10](https://doi.org/10.3847/2041-8205/831/1/L10)
- Goldreich, P., & Julian, W. H. 1969, *ApJ*, 157, 869, doi: [10.1086/150119](https://doi.org/10.1086/150119)
- Goldreich, P., & Lynden-Bell, D. 1969, *ApJ*, 156, 59, doi: [10.1086/149947](https://doi.org/10.1086/149947)
- Hansen, B. M. S., & Lyutikov, M. 2001, *MNRAS*, 322, 695, doi: [10.1046/j.1365-8711.2001.04103.x](https://doi.org/10.1046/j.1365-8711.2001.04103.x)
- Hurley-Walker, N., Zhang, X., Bahramian, A., et al. 2022, *Nature*, 601, 526, doi: [10.1038/s41586-021-04272-x](https://doi.org/10.1038/s41586-021-04272-x)
- Hurley-Walker, N., Rea, N., McSweeney, S. J., et al. 2023, *Nature*, 619, 487, doi: [10.1038/s41586-023-06202-5](https://doi.org/10.1038/s41586-023-06202-5)
- Hurley-Walker, N., McSweeney, S. J., Bahramian, A., et al. 2024, arXiv e-prints, arXiv:2408.15757, doi: [10.48550/arXiv.2408.15757](https://doi.org/10.48550/arXiv.2408.15757)
- Hyman, S. D., Lazio, T. J. W., Kassim, N. E., et al. 2005, *Nature*, 434, 50, doi: [10.1038/nature03400](https://doi.org/10.1038/nature03400)
- Kaplan, D. L., Hyman, S. D., Roy, S., et al. 2008, *ApJ*, 687, 262, doi: [10.1086/591436](https://doi.org/10.1086/591436)
- Katz, J. I. 2022, *Ap&SS*, 367, 108, doi: [10.1007/s10509-022-04146-2](https://doi.org/10.1007/s10509-022-04146-2)
- Lai, D. 2012, *ApJL*, 757, L3, doi: [10.1088/2041-8205/757/1/L3](https://doi.org/10.1088/2041-8205/757/1/L3)
- Laine, R. O., & Lin, D. N. C. 2012, *ApJ*, 745, 2, doi: [10.1088/0004-637X/745/1/2](https://doi.org/10.1088/0004-637X/745/1/2)
- Marsh, T. R., Gänsicke, B. T., Hümmelich, S., et al. 2016, *Nature*, 537, 374, doi: [10.1038/nature18620](https://doi.org/10.1038/nature18620)
- McWilliams, S. T., & Levin, J. 2011, *ApJ*, 742, 90, doi: [10.1088/0004-637X/742/2/90](https://doi.org/10.1088/0004-637X/742/2/90)
- Melrose, D. B. 2017, *Reviews of Modern Plasma Physics*, 1, 5, doi: [10.1007/s41614-017-0007-0](https://doi.org/10.1007/s41614-017-0007-0)
- Piro, A. L. 2012, *ApJ*, 755, 80, doi: [10.1088/0004-637X/755/1/80](https://doi.org/10.1088/0004-637X/755/1/80)
- Rea, N., Coti Zelati, F., Dehman, C., et al. 2022, *ApJ*, 940, 72, doi: [10.3847/1538-4357/ac97ea](https://doi.org/10.3847/1538-4357/ac97ea)
- Rea, N., Hurley-Walker, N., Pardo-Araujo, C., et al. 2024, *ApJ*, 961, 214, doi: [10.3847/1538-4357/ad165d](https://doi.org/10.3847/1538-4357/ad165d)
- Twiss, R. Q. 1958, *Australian Journal of Physics*, 11, 564, doi: [10.1071/PH580564](https://doi.org/10.1071/PH580564)
- Wadiasingh, Z., Beniamini, P., Timokhin, A., et al. 2020, *ApJ*, 891, 82, doi: [10.3847/1538-4357/ab6d69](https://doi.org/10.3847/1538-4357/ab6d69)
- Wang, J.-S., Yang, Y.-P., Wu, X.-F., Dai, Z.-G., & Wang, F.-Y. 2016, *ApJL*, 822, L7, doi: [10.3847/2041-8205/822/1/L7](https://doi.org/10.3847/2041-8205/822/1/L7)
- Wu, C. S., & Lee, L. C. 1979, *ApJ*, 230, 621, doi: [10.1086/157120](https://doi.org/10.1086/157120)
- Wu, K., Cropper, M., Ramsay, G., & Sekiguchi, K. 2002, *MNRAS*, 331, 221, doi: [10.1046/j.1365-8711.2002.05190.x](https://doi.org/10.1046/j.1365-8711.2002.05190.x)

Table 1. Published LPRTs with measured periods, luminosities, polarization degrees and possible optical counterparts. AR Scorpii is also included because of its possible similar origin.

Source	P (min)	Π_L (%)	Optical counterparts	Reference
GCRT J1745–3009	77	/	No detection	Hyman et al. (2005) ; Kaplan et al. (2008)
GLEAM-X J1627-52	18.18	88 ± 1	No detection	Rea et al. (2022) ; Hurley-Walker et al. (2022)
GPM J1839-10	21	10–100	KD or MD?	Hurley-Walker et al. (2023)
ASKAPJ193505.1+214841.0	53.8	> 90	near IR source ?	Caleb et al. (2024)
ILT J1101 + 5521	125.5	51 ± 6	WD+MD	de Ruiter et al. (2024)
GLEAM-X J 0704-37	174	20–50	MD	Hurley-Walker et al. (2024)
AR Scorpii	213.6	/	WD+MD	Marsh et al. (2016)

Zhang, B. 2023, *Reviews of Modern Physics*, 95, 035005,

doi: [10.1103/RevModPhys.95.035005](https://doi.org/10.1103/RevModPhys.95.035005)

Zhang, B., & Gil, J. 2005, *ApJL*, 631, L143, doi: [10.1086/497428](https://doi.org/10.1086/497428)

Zhu, W. W., & Xu, R. X. 2006, *MNRAS*, 365, L16,

doi: [10.1111/j.1745-3933.2005.00117.x](https://doi.org/10.1111/j.1745-3933.2005.00117.x)